

Investigation of cell morphology by the TRUImagE digital holographic microscopy system

Chee, Oi Choo; Qu, Weijuan; Chai, Kim Kheong; Asundi, Anand Krishna

2012

Chee, O. C., Qu, W., Chai, K. K., & Asundi, A. K. (2012). Investigation of cell morphology by the TRUImagE digital holographic microscopy system. Proceedings of SPIE - Biophotonics: Photonic Solutions for Better Health Care III, 84272G.

<https://hdl.handle.net/10356/98143>

<https://doi.org/10.1117/12.921613>

© 2012 SPIE. This paper was published in Proceedings of SPIE - Biophotonics: Photonic Solutions for Better Health Care III and is made available as an electronic reprint (preprint) with permission of SPIE. The paper can be found at the following official DOI: [<http://dx.doi.org/10.1117/12.921613>]. One print or electronic copy may be made for personal use only. Systematic or multiple reproduction, distribution to multiple locations via electronic or other means, duplication of any material in this paper for a fee or for commercial purposes, or modification of the content of the paper is prohibited and is subject to penalties under law.

Downloaded on 20 Mar 2024 17:05:40 SGT

Investigation of cell morphology by the *TRUImage* digital holographic microscopy system

Chee Oi Choo ^{*a}, Qu Weijuan ^a, Chai Kim Kheong ^b, and Anand Asundi^c

^aSchool of Engineering, Ngee Ann Polytechnic, 535 Clementi Road, Singapore 599489

^bSchool of Life Sciences and Chemical Technology, Ngee Ann Polytechnic,
535 Clementi Road, Singapore 599489

^cSchool of Mechanical and Aerospace Engineering, Nanyang Technological University,
50 Nanyang Avenue, Singapore 639798

ABSTRACT

We report the development of the *Three-dimensional Real-time Uninvasive Imaging and Evaluation (TRUImage)* system based on digital holographic microscopy to study the morphological changes in cells undergoing photodynamic therapy-induced cell death. The optical system, based on the Michelson interferometer and configured in transmission mode, and the sample holder incorporating a stage incubator have been developed for monitoring various tumorigenic cell samples without the use of markers. Off-axis digital holograms were recorded with a CCD sensor and numerically reconstructed to provide quantitative phase imaging and 3D morphology of the cells in real time. The system was used to continuously monitor and study, at different time points, the changes in cells after incubation with the photosensitizer followed by activation by the appropriate light dose. Results obtained from the *TRUImage* system and biochemical assays will be given.

Keywords: Digital holographic microscopy, quantitative phase imaging, cell morphology, photodynamic therapy

1. INTRODUCTION

Morphological criteria have been used to distinguish different modes of cell death, namely, apoptosis, autophagy, and necrosis^{1, 2, 3}. Each has its own distinctive features. Apoptosis occurs with a reduction in cellular size, nuclear fragmentation, and breaking into apoptotic bodies. Autophagy is characterised by the formation of autophagic vacuoles in the cytoplasm and degradation by lysosomes. Necrosis is characterised by swelling of the cell, loss of plasma membrane integrity, and release of the cytoplasm to the surrounding. The spatial reorganisation of the cellular components do not show up well under normal illumination and various phase imaging microscopes have been developed which exploit the optical phase shift introduced to the incident light wavefront caused by variations in the refractive index of the cell and its internal structures. Digital holographic microscopy (DHM) has generated much interest as this technique can provide direct quantitative evaluation of the phase changes^{4, 5, 6}.

*coc@np.edu.sg

The phase change φ is related to the cell thickness h , integral refractive index of the cell n_c , refractive index of the surrounding medium n_s , and wavelength of the light source λ by:

$$h(x, y) = \frac{\lambda}{2\pi} \frac{\varphi(x, y)}{(n_c - n_s)} \quad (1)$$

In our study, we have developed the *Three-dimensional Real-time Uninvasive Imaging and Evaluation (TRUImageE)* system based on DHM and investigated cell death mediated by photodynamic therapy (PDT). PDT, a relatively novel approach to treat a variety of tumours and diseases characterised by abnormal cell growth, uses a photosensitizing drug, followed by irradiation with light of an appropriate wavelength, to induce cell death⁷. The selective uptake of the photosensitizing drug in the tumour cells kills them without damaging surrounding healthy ones. One of the most effective and extensively-studied photosensitizer is hypericin which is a natural pigment isolated from plants of the genus *Hypericum*^{7, 8, 9}.

2. DESCRIPTION OF THE *TRUImageE* SYSTEM

Figure 1 shows the schematic and actual *TruImageE* system based on the Michelson interferometer in transmission mode with physical phase compensation which we have developed and reported previously^{10, 11}. The light source is coupled to the system via a fiber optic splitter. Light from fiber point 1 together with a condenser provides the object wave. A microscope objective (Mitutoyo infinity-corrected long-working distance objective, 50 \times , 0.55 NA) together with a tube lens performs the imaging of the test object. Light from fiber point 2 provides the reference wave and the wavefront is determined by the position of the fiber point. The object and reference waves interfere at the beam splitter, resulting in an off-axis hologram which is captured by the CCD sensor (4.65 μm x 4.65 μm). The sample holder incorporates a stage incubator to maintain the required environmental conditions to enable prolonged observations of live cell samples. The input light source is changeable between two laser diode modules of different wavelengths: 640 nm and 785 nm. When monitoring cells treated with hypericin-PDT, the latter is used since it is outside the light activation wavelength bands for the photosensitizer.

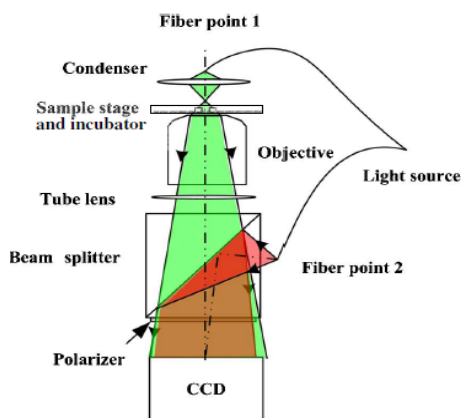
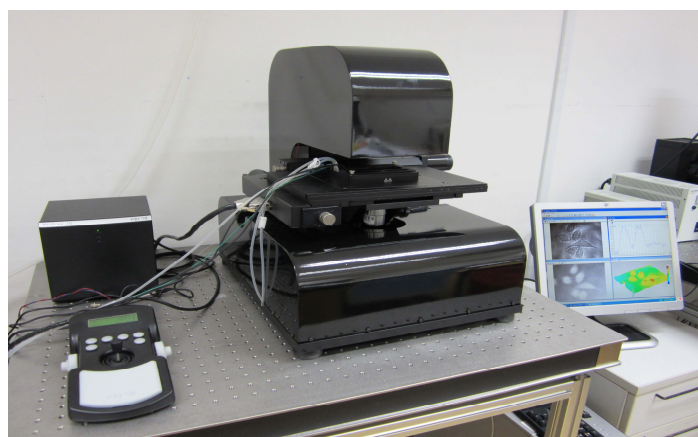


Figure 1(a) Schematic of setup



(b) *TruImageE* system

3. MATERIALS AND METHODS

3.1. Cell culture

Human nasopharyngeal carcinoma cell line CNE2 was kindly provided by the Singapore National Cancer Centre^{8,9} and cultured in Roswell Park Memorial Institute (RPMI)1640 medium (Invitrogen, Carlsbad, CA) supplemented with 10% fetal bovine serum, 2 mM glutamine, 1mM non-essential amino acids, 1 mM sodium pyruvate, and 100 U/ml penicillin in a 5% CO₂, 95% air, 37°C humidified incubator.

3.2. Photodynamic therapy

A stock solution of hypericin (Molecular Probes, Eugene, OR) was prepared in dimethyl sulfoxide (DMSO) at a concentration of 1 mg/ml. CNE2 cells were cultured in T₂₅ flasks and seeded with 5x10⁵ cells. 1.25 µM hypericin was diluted from the stock and added to the flasks (except for one used as control) and incubated in the dark for 16 hours. The medium was replaced with hypericin-free medium and the flasks were irradiated with a light dose of 0.5 J/cm² in the 580-620 nm band. The fluence rate was measured using a power meter (LaserCheck, Coherent, USA). The flasks were placed in the incubator and taken out at different hours after PDT for biochemical tests to assess the biochemical aspects involved.

3.3. Digital holographic microscopy

For observation with DHM, the CNE2 cells were seeded in Lab-Tek[®] chamber slides. The chamber slide was placed on the stage incubator (humidified air with 5% CO₂ at 37°C) of the *TRUImagE* system and monitored continuously. Images of the cells were recorded before PDT and at a 2-min interval for 24 hours after PDT.

3.4. Detection of activated caspases

CaspGLOW[™] fluorescein active caspase/caspase-3/caspase-8/caspase-9 staining kits (BioVision, Mountain View, CA) were used to evaluate the presence of active caspases according to the manufacturer's instructions. The FITC-conjugated caspase inhibitors used were VAD-FMK for the caspase family, DEVD-FMK for caspase-3, IETD-FMK for caspase-8, and LEHD-FMK for caspase-9. Flasks were taken out from the incubator at 0 hr., 1 hr., 2hr, and 24 hr. after PDT. Cells were collected and resuspended in RPMI and incubated with the FITC-conjugated caspase inhibitor. Cells were then collected and viewed under a fluorescent microscope (Olympus IX71, Tokyo, Japan) to assess the activation of caspases.

3.5. Detection of phosphatidylserine exposure and plasma membrane rupture

Annexin V-Biotin apoptosis detection kit (BioVision, Mountain View, CA) combined with nuclear yellow (Molecular Probes, Eugene, OR) was used to detect phosphatidylserine (PS) exposure and plasma membrane rupture. A flask was taken out from the incubator at 0 hr., 1 hr., 2 hr., 3 hr., and 24 hr. after PDT. Cells were collected and resuspended in Annexin-V binding buffer according to the manufacturer's instructions and incubated with Annexin V-Biotin and nuclear yellow. Cells were fixed with 2% formaldehyde and incubated with avidin-fluorescein. Cells were then collected and

viewed under the fluorescent microscope to assess Annexin-V binding and nuclear yellow staining of permeabilised cells.

3.6. Detection of nuclear condensation

A flask was taken out from the incubator at 0 hr., 3 hr., 5 hr., and 24 hr. after PDT. Cells were stained with 4, 6-Diamidino-2-phenylindole (DAPI) purchased from Sigma-Aldrich (St Louis, MO) and viewed under the fluorescent microscope to examine the nuclear chromatin.

4. RESULTS AND DISCUSSION

Figure 2 shows the quantitative phase images of CNE2 cells obtained from the *TruImage* system before PDT and at different time points after PDT. The phase profiles along the line drawn across cells C, D, and E are shown in Figure 3.

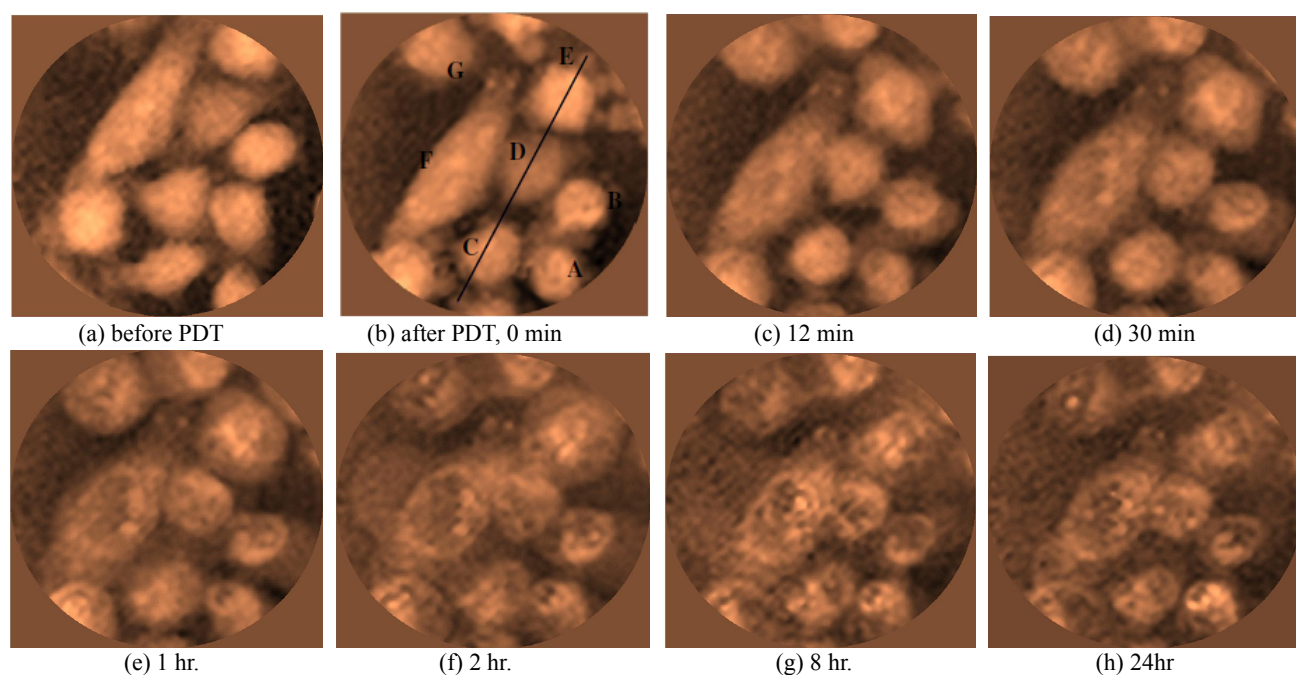


Figure 2. Quantitative phase images of CNE cells

From Figure 2, blebs were seen to start forming on the cells immediately after PDT. For cells A and B, areas of a higher phase value were noticed after 2 hr. and became increasingly more pronounced until the 24 hr. These were probably due to the condensation of nuclear chromatin. On the other hand, cells F and G began to swell 1 hr. after PDT and their plasma membrane seemed permeabilised after 2 hr.

Referring to Figures 2 and 3, it was noticed that cell C reduced in size for 30 min and flattened gradually until the 8th hour when two areas of high phase values became noticeable and remained about the same until the 24th hour. Cells D and E changed pronouncedly during the first 12 min. For cell D, areas of a higher phase value appeared and remained about the same until the 24 hr. On the contrary, cell E appeared to flatten until the 8th hour when the plasma membrane

appeared permeabilised. Finally, after 24 hours, most of the cells appeared to have lysed.

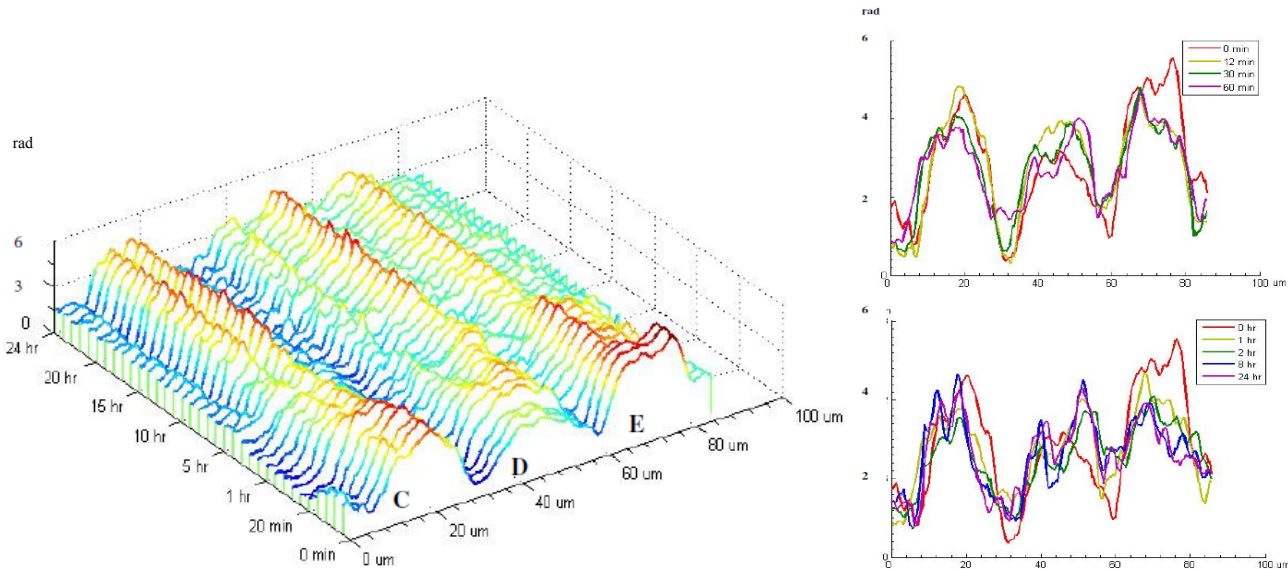


Figure 3. Phase profile along the line drawn across cells C, D, and E (a) 0-24 hours (b) 0-60 min (c) 0, 1, 2, 8, 24 hr. after PDT

Figures 4, 5, and 6 show the results for the biochemical assay tests for caspase activation, PS expression and cell viability, and chromatin condensation respectively. 300 cells were randomly chosen and counted and the tests were repeated for each assay.

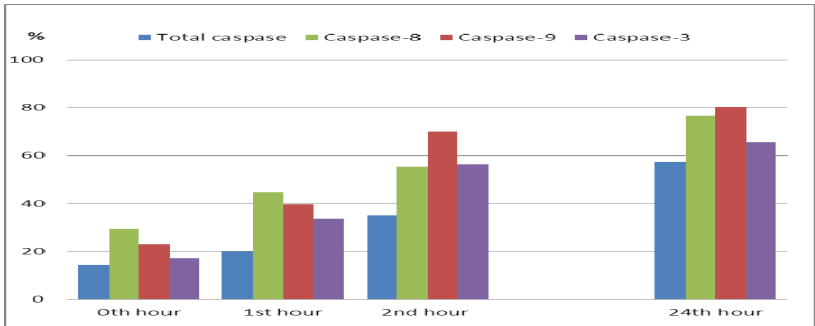


Figure 4. Percent of cells with activated caspase, caspase-8, caspase-9, and caspase-3

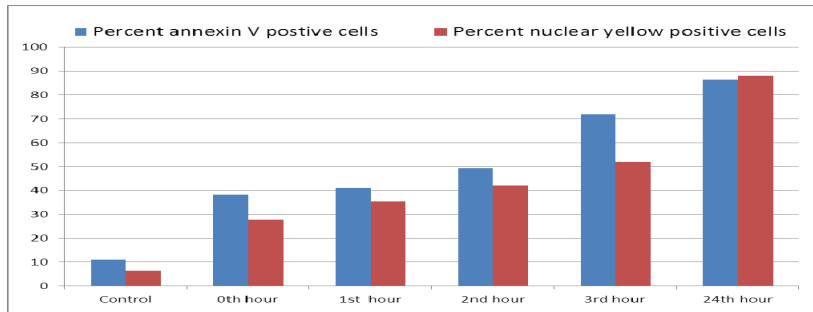


Figure 5. Percent annexin-V positive and nuclear yellow positive cells.

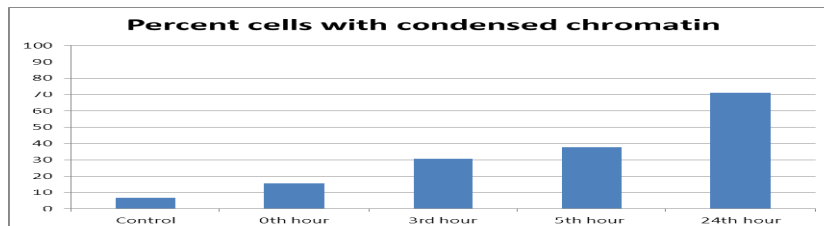


Figure 6. Percent of cells with condensed chromatin detected by DAPI staining

The number of cells tested positive for the total caspase, caspase-8, caspase-9, and caspase-3 increased with time suggesting that more cells became apoptotic with time after PDT treatment. It appeared that both the extrinsic-pathway caspase-8 and intrinsic-pathway caspase-9 were involved in initiating the activity of effector caspase-3. 50% of the cells appeared to show caspase-3 activity and commitment to apoptosis by the 2nd hour.

Annexin-V binds to PS exposed on the outer leaflet of the plasma membrane before DNA fragmentation during apoptosis and nuclear yellow localises in the nucleus of permeabilised cells. From Figure 5, there was a time lag between PS exposure and cell permeability during apoptosis. The events coincided after 24 hours. Most of the cells had lysed and the contents of their cytoplasm were released to the surrounding. Independent assessment of cell viability with trypan blue also yielded comparable results (not shown here) to nuclear yellow staining. Figure 6 shows the proportion of cells with condensed chromatin increasing in a similar fashion following PS expression.

In conclusion, DHM is able to monitor the quantitative phase information of live cell samples continuously and capture rapid and subtle changes that occur. The morphological features provided by DHM and the biochemical results indicate that both the apoptotic and necrotic modes of cell death were induced by the PDT tests carried out in our study. Both results show good agreement.

ACKNOWLEDGEMENTS

This study was supported by Innovation Fund grant MOE2008-IF-1-009 from the Singapore Ministry of Education and Translational Research & Development grant NRF2009NRF-TRD001-008 from the Singapore National Research Foundation. The authors thank Mr Lewis Tan for performing the experiments, Mr Wang Zhaomin for developing the software, and Ms Ramaswamy Bhuvaneswari of the Singapore National Cancer Centre for assisting with the PDT protocol.

REFERENCES

- [1] Kroemer, G., Galluzzi, L., Vandenabeele, P., Abrams, J., Alnemri, E.S., Baehrecke, E. H., Blagosklonny, M. V., El-Deiry, W.S., Golstein, P., Green, D.R., Hengartner, M., Knight, R.A., Kumar, S., Lipton, S.A., Malorni, W., Nuñez, G., Peter, M.E., Tschopp, J., Yuan, J., Piacentini, M., Zhivotovsky, B., and Melino, G., "Classification of cell death: recommendations of the Nomenclature Committee on Cell Death 2009," *Cell Death and Differentiation* 16, 3-11 (2009).
- [2] Fink, S.L. and Cookson, B.T., "Apoptosis, pyroptosis, and necrosis: mechanistic description of dead and dying eukaryotic cells," *Infection and Immunity* 73 (4), 1907-1916 (2005).
- [3] Rello, S., Stockert, J.C., Moreno, V., Gamez, A., Pacheco, M., Juarranz, A., Cañete, M., and Villanueva, A., "Morphological criteria to distinguish cell death induced by apoptotic and necrotic treatments," *Apoptosis* 10 (1), 201-208 (2005).
- [4] Kemper, B. and von Bally, G., "Digital holographic microscopy for live cell applications and technical inspection," *Appl. Opt.* 47 (4), A52-A61 (2008).
- [5] Alm, K., Cirenajwis, H., Gisselsson, L., Gjörlöf Wingren, A., Janicke, B., Mölder, A., Oredsson, S., and Persson, J., "Digital Holography and Cell Studies," [Holography, Research and Technologies, Rosen J. (Ed.)] InTech, Rijeka, 237-252 (2011).
- [6] Colomb, T., Charrirere, F., Kühn, J., Marquet, P., and Depeursinge, C., "Advantages of digital holographic microscopy for real-time full field absolute phase imaging," *Proc. of SPIE* 6861, (2008).
- [7] Oleinick, N.L., Morris, R.L., and Belichenko, I., "The role of apoptosis in response to photodynamic therapy: what, where, why, and how," *Photochem. Photobiol. Sci.* 1, 1-21 (2002).
- [8] Ali, S.M., Olivo, M., Gan, Y.Y., and Soo, K.C., "Induction of apoptosis by hypericin through activation of caspase-3 in human carcinoma cells," *Int. J. Mol. Medicine* 8, 521-530 (2001).
- [9] Du, H.Y., Li, Y., Olivo, M., Yip, G.W.C., and Bay, B.H., "Differential up-regulation of metallothionein isoforms in well-differentiated nasopharyngeal cancer cells in vitro by photoactivated hypericin," *Oncology Reports* 16, 1397-1402 (2006).
- [10] Qu, W., Chee, O.C., Singh, V. R., Yu Y., and Asundi, A., "Quasi-physical phase compensation in digital holographic microscopy," *J. Opt. Soc. Am. A* 26 (9), 2005-2011 (2009).
- [11] Qu, W., Chee, O.C., Yu Y., and Asundi, A., "Microlens characterization by digital holographic microscopy with physical spherical phase compensation," *Appl. Opt.* 49 (33), 6448-6454 (2010).